Pet. Sci. (2017) 14:50–60
DOI 10.1007/s12182-016-0147-9

ORIGINAL PAPER

Features and genesis of Paleogene high-quality reservoirs in lacustrine mixed siliciclastic–carbonate sediments, central Bohai Sea, China

Zheng-Xiang Lü[1,2] · Shun-Li Zhang[1] · Chao Yin[1] · Hai-Long Meng[1] · Xiu-Zhang Song[1] · Jian Zhang[1]

Received: 25 February 2016 / Published online: 21 January 2017

Abstract The characteristics and formation mechanisms of the mixed siliciclastic–carbonate reservoirs of the Paleogene Shahejie Formation in the central Bohai Sea were examined based on polarized light microscopy and scanning electron microscopy observations, X-ray diffractometry, carbon and oxygen stable isotope geochemistry, and integrated fluid inclusion analysis. High-quality reservoirs are mainly distributed in Type I and Type II mixed siliciclastic–carbonate sediments, and the dominant pore types include residual primary intergranular pores and intrafossil pores, feldspar dissolution pores mainly developed in Type II sediments. Type I mixed sediments are characterized by precipitation of early pore-lining dolomite, relatively weak mechanical compaction during deep burial, and the occurrence of abundant oil inclusions in high-quality reservoirs. Microfacies played a critical role in the formation of the mixed reservoirs, and high-quality reservoirs are commonly found in high-energy environments, such as fan delta underwater distributary channels, mouth bars, and submarine uplift beach bars. Abundant intrafossil pores were formed by bioclastic decay, and secondary pores due to feldspar dissolution further enhance reservoir porosity. Mechanical compaction was inhibited by the precipitation of pore-lining dolomite formed during early stage, and oil emplacement has further led to the preservation of good reservoir quality.

Keywords High-quality reservoirs · Mixed sediments · Paleogene Bohai Sea

1 Introduction

In addition to carbonate and clastic reservoir rock types, magmatic, metamorphic, shale and mixed siliciclastic–carbonate sedimentary reservoirs can also be considered as important targets for oil and gas exploration and development (Ge et al. 2011; Tong et al. 2012; Xiao et al. 2015; Palermo et al. 2008). The concept of "mixed sediments" was firstly proposed by Mount (1984) and is commonly referred to as sediments that are composed of mixtures of siliciclastic and carbonate material (including allochemical particles) (Lubeseder et al. 2009; Brandano et al. 2010; Xu et al. 2014). Many Chinese and foreign scholars have made in-depth studies of the formation mechanisms of this type of sediment and suggested that it can be developed in both marine and lacustrine environments. Influenced by sea (lake)-level fluctuations, structural changes, storm, current and tidal actions, mixed siliciclastic–carbonate sediments are widely distributed in transitional marine-terrestrial, continental shelf, and slope environments (García-Hidalgo et al. 2007; Zonneveld et al. 2012). Under certain conditions, mixed siliciclastic–carbonate sediments may be rich in oil and gas. For example, hydrocarbon accumulations have been discovered in the high-quality mixed siliciclastic–carbonate reservoirs in China, such as the Bohai Bay Basin, the Qaidam Basin and the Sichuan Basin (Feng et al. 2011a, b, 2013; Zhang et al. 2006; Liu et al. 2011; García-Hidalgo et al. 2007). Although carbonate and clastic

✉ Shun-Li Zhang
1205799554@qq.com

[1] College of Energy Resources, Chengdu University of Technology, Chengdu 610059, Sichuan, China

[2] State Key Laboratory of Oil-Gas Reservoirs Geology and Exploitation, Chengdu University of Technology, Chengdu 610059, Sichuan, China

Edited by Jie Hao

reservoirs have been the subject of intensive study by a large number of researchers, mixed siliciclastic–carbonate reservoirs have received less attention. Previously, studies of mixed siliciclastic–carbonate reservoirs have mainly focused on petrography, structure, classification, the establishment of depositional models (Caracciolo et al. 2012; Sha 2001; Zand-Moghadam et al. 2013; Zonneveld et al. 2012; Ma and Liu 2003), and the reconstruction of the sedimentary environment on the basis of sequence stratigraphy, sea level change and paleoclimate (Anan 2014; Campbell 2005; Moissette et al. 2010). However, the microscopic features and the formation mechanisms of high-quality reservoirs have not been well investigated, which has restricted the exploration and development of mixed siliciclastic–carbonate reservoirs.

The Bohai Bay Basin is an important petroliferous basin in North China. In the Paleogene, steep slope zones were well developed and are represented by a series of high steep fault noses (Lu 2005; Guan et al. 2012). The tectonically induced physiographic changes controlled the distribution and areal extension of mixed siliciclastic–carbonate sediments. For example, typical mixed sediments composed of lacustrine carbonate and siliciclastic material are widely distributed in the Shijiutuo Uplift in the central basin, and a large number of high-quality reservoirs are developed in them (Liu et al. 2011; Song et al. 2013). Statistics suggest that reservoir quality is one of the key controls on prospectivity during petroleum exploration and production. The study of the characteristics and formation mechanisms of mixed siliciclastic–carbonate reservoirs is therefore of significant importance for guiding the oil and gas exploration and production in the Bohai Sea. The purpose of this paper is to compare different types of mixed siliciclastic–carbonate reservoirs, to describe the main features of high-quality reservoirs, and to determine the formation mechanisms of high-quality reservoirs by integrating geological and geochemical data.

2 Geological setting

The Bohai Bay Basin is a Cenozoic rift basin superimposed on the Paleozoic basement of the North China platform (Lu 2005). The study area is located in the Shijiutuo Uplift in the central Bohai Bay Basin and bounded by two large hydrocarbon generation sags—Bozhong Sag and Qin'nan Sag (Fig. 1). The hydrocarbon accumulation condition is excellent with high-quality source rocks and a series of Paleogene high steep fault nose traps developed (Guan et al. 2012). The mixed sedimentary reservoirs in the study area are mainly developed in the Paleogene Shahejie Formation (E_2s). The Shahejie Formation is 300–400 m thick with burial depths >3000 m and conformably overlies the Kongdian Formation (E_2k) and underlies the Dongying Formation (E_2d). Because economically significant hydrocarbon accumulations have been found in the mixed reservoirs, the mixed siliciclastic–carbonate reservoirs have been the focus of study in recent years (Wang et al. 2015).

3 Samples and experimental methodology

In this study, 240 mixed siliciclastic–carbonate sediment samples from 12 wells in the Shijiutuo Uplift in the central Bohai Bay Basin, such as Well HD2 and Well HD5, were selected for porosity and permeability measurements. The locations of sample wells are shown in Fig. 1. The microscopic features, such as petrology, pore space types, and diagenesis, were obtained from 122 thin sections with different physical properties. Multi-purpose thin sections were prepared with blue-dyed epoxy impregnation and double-sided polishing. The mineral composition was identified by polarized light microscopy, and X-ray diffraction (XRD) analyses were carried out on twenty-two bulk samples and <2 μm size fractions using a Rigaku DMAX-3C diffractometer. The chemical composition of grain-coating and dissolved minerals was determined quantitatively by electron microprobe analysis (EMPA) using a Shimadzu EPMA-1720 and a JEOL JXA-8100 electron microprobes (operating conditions: 15 kV accelerating voltage, 10 mA current, 1 μm beam diameter). Fifteen double-thickness polished thin sections were selected for microthermometric measurements. Homogenization temperatures were measured using a Linkam THMS-600 heating/cooling stage. Only primary fluid inclusions with both aqueous and hydrocarbon phases were selected from authigenic minerals to determine their minimum precipitation temperatures (Liu et al. 2005; Lü et al. 2015; Guo et al. 2012; Tian et al. 2016). In-situ carbon and oxygen isotope analysis was performed using an Nd:YAG laser microprobe. Laser probe microsampling of C and O from carbonate cements for isotopic analysis was achieved by focusing a laser beam with a wavelength of 1064 nm and a diameter of 20 μm onto a sample situated in a vacuum chamber to ablate a small area on the sample and liberate CO_2 gas. After purification, the CO_2 gas was led directly into a Finnigan MAT 252 mass spectrometer for isotopic analysis. After obtaining the isotopic values, the dolomite formation temperature (T) was calculated using the empirical formula proposed by Hu et al. (2012):

$$T = 16.5 - 4.3(\delta C - \delta W) + 0.14(\delta C - \delta W)(\delta C - \delta W)$$

where δC is the $\delta^{18}O$ of a dolomite precipitate, and δW is the $\delta^{18}O$ of parent water.

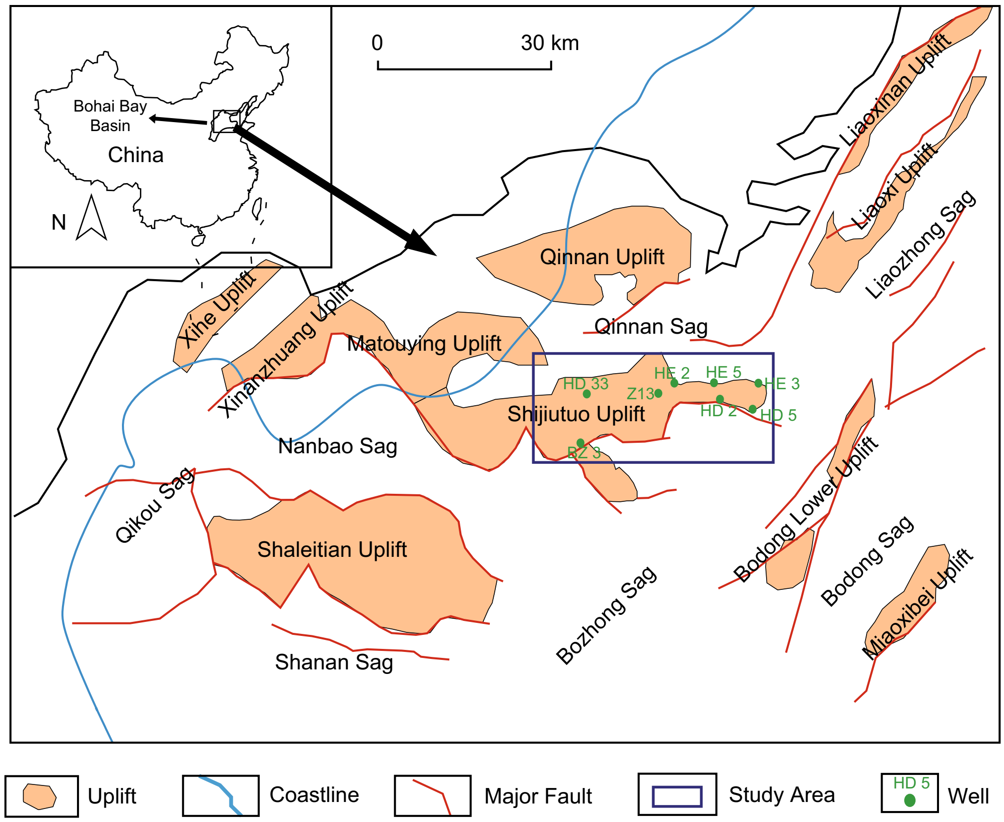

Fig. 1 Location map and tectonic elements of the central Bohai Sea

The timing of feldspar dissolution was mainly determined based on the fluid inclusion temperatures of the dissolution products (authigenic quartz). Sixty-two samples were observed under a DM4500P fluorescence microscope in order to identify possible petroleum inclusions. Fifteen inclusions were also examined using a Renishaw inVia laser Raman microprobe with a wavelength of 514.5 nm to document the existence of hydrocarbons.

The mixed siliciclastic–carbonate sediments were deposited in a fan delta environment (Guan et al. 2012; Zhang et al. 2015; Ni et al. 2013). In order to illustrate the relationship between petrophysical properties and sedimentary microfacies, the sedimentary facies were identified by analyzing rock textures and well log data for Well HD2 and Well HD5, in which core porosity and permeability were measured.

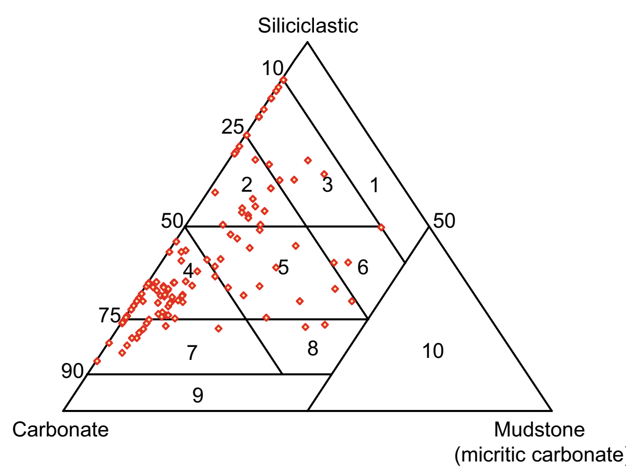

Fig. 2 Rock types of E_2s mixed siliciclastic–carbonate sediments. 1: sand (gravel) rock, 2: carbonate siliciclastic mixed sedimentary rocks, 3: carbonate-bearing siliciclastic mixed sedimentary rocks, 4: siliciclastic carbonate mixed sedimentary rocks, 5: carbonate/siliciclastic mixed sedimentary rocks, 6: carbonate-bearing argillaceous siliciclastic mixed sedimentary rocks, 7: siliciclastic-bearing carbonate mixed sedimentary rocks, 8: siliciclastic-bearing micrite carbonate mixed sedimentary rocks, 9: carbonate, 10: mudstone (micritic carbonate)

4 Results

4.1 Rock types

The E_2s mixed sediments are composed of siliciclastic and lacustrine carbonate rocks. For the siliciclastic grains, carbonate grains, matrix, and micrite that constituted the mixed sediments, the content of the former two was, respectively, not less than 10%, while the latter two accounted for less than 50%. The identification results of

122 thin sections show that (Fig. 2) E_2s mixed siliciclastic–carbonate sediments were divided into three classes. Class I was mainly composed of siliciclastic carbonate mixed sedimentary rocks and siliciclastic-bearing carbonate mixed sedimentary rocks. It represented up to 55% with carbonate particles content of more than 50% (4, 7 area in Fig. 2). Carbonate grains were mainly bioclasts, accounting for 65% (103 sampling points), followed by oolites and arenes; Class II was mainly composed of carbonate siliciclastic mixed sedimentary rocks and carbonate-bearing siliciclastic mixed sedimentary rocks, accounting for 30%, with siliciclastic particles content of more than 50% (2, 3 area in Fig. 2); Class III was uniformly with less than 50% of siliciclastic grains and of carbonate grains (5, 6 and 8 area in Fig. 2). It was in the lowest content, only accounting for 16%. The interstitial material was mainly dolomite, followed by calcite and small amounts of argillaceous matrix, which was well-sorted and sub-rounded to rounded.

4.2 Diagenetic features

4.2.1 Compaction

From the contact relationship of grains in E_2s mixed siliciclastic–carbonate sediments, it showed that the compaction was not strong, mainly composed of point-line contact (Fig. 3a, b).

4.2.2 Precipitation of authigenic minerals

There were numerous types of authigenic minerals formed in E_2s mixed siliciclastic–carbonate sediments. As with the different proportions of siliciclastics and carbonate, it led to the differences of authigenic mineral content in the mixed siliciclastic–carbonate sediments. In the mixed siliciclastic–carbonate sediments with a high proportion of carbonate, authigenic dolomite, calcite and other carbonate minerals were in high proportions and authigenic clay was in small proportions. However, in the mixed siliciclastic–carbonate sediments with a high proportion of siliciclastic rocks, the authigenic minerals were dominated by kaolinite, illite, and quartz, and the authigenic carbonate minerals were in minor amounts.

Among authigenic carbonate minerals, dolomite made up the largest share, followed by calcite; in addition, there were minor amounts of ankerite and ferroan calcite. The occurrence states of dolomites were a pore liner (Fig. 3a), pore fillings (Fig. 3a, c) and replacement particles (Fig. 3d, e). Calcite mainly occurred as local replacement particles. Authigenic clay minerals included kaolinite (Fig. 3f) and a small amount of illite (Fig. 3f). Authigenic quartz was distributed in the pores in the form of small crystals (Fig. 3f), and pyrite can be occasionally seen.

4.2.3 Dissolution

Dissolution was well developed in the E_2s mixed siliciclastic–carbonate sediments, and it effectively improved the quality of reservoirs with high proportion of siliciclastic rocks. The dissolved minerals were mainly feldspar, especially albite and K-feldspar (Fig. 3d, e). A small amount of carbonate minerals, such as dolomite and ankerite, were dissolved but this made little contribution to pores.

4.3 Reservoir space features

The reservoir space of E_2s mixed siliciclastic–carbonate sediments was dominated by residual primary intergranular pores and dissolved pores, with minor intercrystalline porosity. Primary pores mainly included residual primary intergranular pores and intrafossil pores (Fig. 3a). Dissolved pores mainly included intergranular dissolved pores in feldspars and rock fragments (Fig. 3d) and intercrystalline pores mainly included intercrystalline pores in kaolinite (Fig. 3f).

4.4 Petrophysical features

The porosity of E_2s mixed siliciclastic–carbonate sediments ranged between 0.45% and 36%. In the 240 samples, 76% samples had a porosity of over 15% (Fig. 4). Permeability mainly ranged between 0.014 and 11259 mD. Most samples had a permeability of over 10 mD, accounting for 53% of the total samples (Fig. 5).

4.5 Features of sedimentary microfacies

The E_2s in the study area was deposited in a continental offshore lacustrine and near-source fan delta depositional environment (Guan et al. 2012; Zhang et al. 2015; Ni et al. 2013). The mixed siliciclastic–carbonate sediments were mainly developed in delta front sandbars and shallow lacustrine underwater uplift beach bars, followed by delta front underwater distributary channels. Front sandbars were divided into mouth bar and distal bar microfacies with reverse grain size grading and funnel-shaped gamma-ray (*GR*) curves, but the former showed lower *GR* curves. Underwater uplift beach bars were characterized by fine grain size, good sorting, low content of matrix and micrite and a box-shaped *GR* curve. Underwater distributary channels abruptly contacted with underlying strata, with coarse grain size at the bottom and minor gravel (Fig. 6).

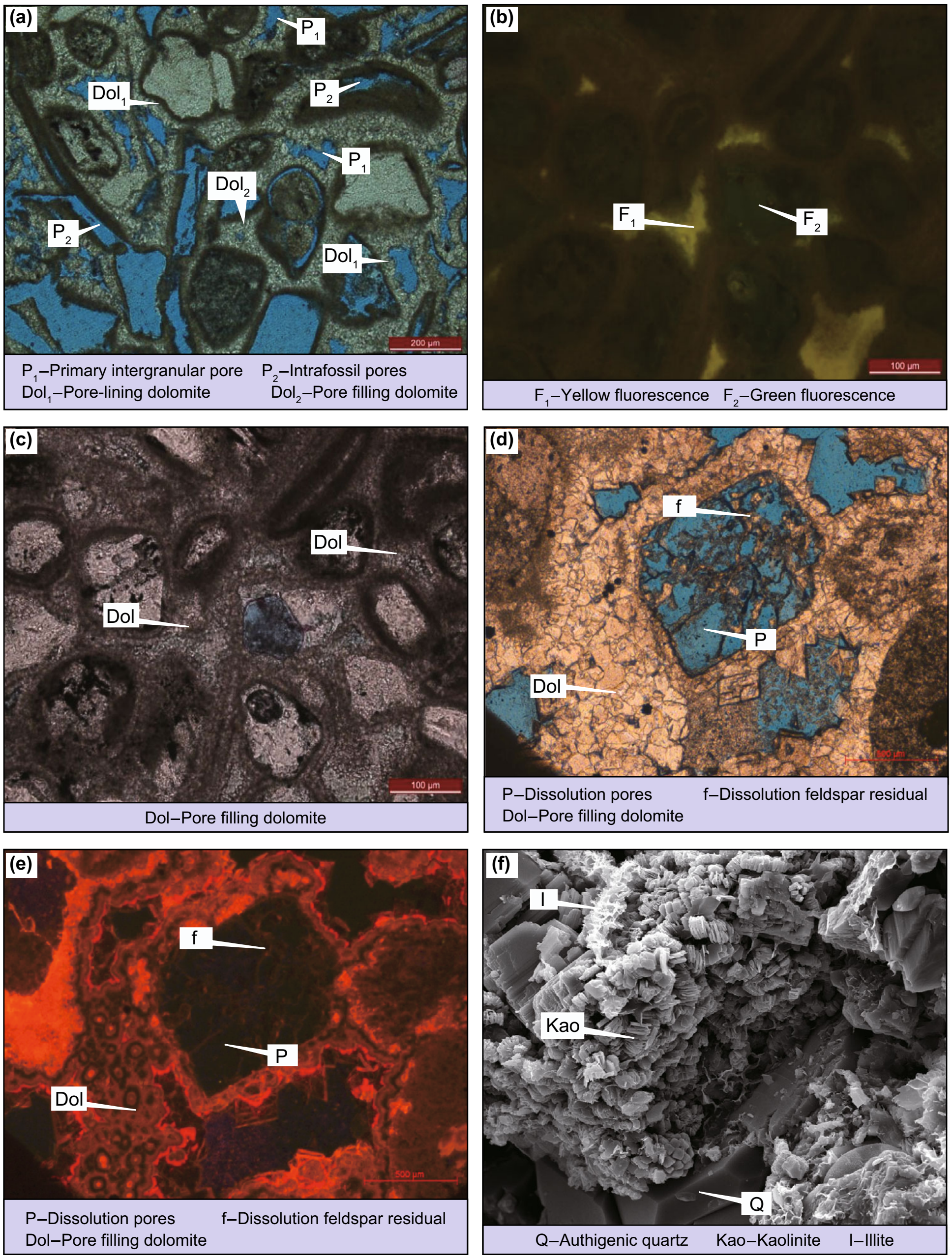

Fig. 3 Photomicrographs of **a** residual intergranular primary pore and intrafossil pores, pore-lining dolomite and filling dolomite, point-line contact, Well HD2, 3762.6 m, polarized light. **b** Two phases of hydrocarbon charging in intergranular dissolved pores and residual intergranular primary pore, Well HD2, 3774.33 m, fluorescence microscope. **c** Pore filling dolomite, pore is poorly developed, Well HD2, 3774.33 m, polarized light. **d** Multiphased authigenic dolomite, dolomite replaces feldspar, feldspar (EPMA: Na_2O: 0.2%, K_2O: 16.5%, Al_2O_3: 18.3%, SiO_2: 64.6%) dissolution, Well HD5, 3382.1 m, polarized light. **e** multiphased authigenic dolomite, dolomite replaces feldspar, feldspar dissolution, Well HD5, 3382.1 m, Cathodoluminescence. **f** Kaolinite, authigenic quartz, illite, Well HD5, 3486.5 m, Scanning electron microscope

According to the sedimentary microfacies and the statistics of components in the 156 samples, the content of siliciclastic particles decreased from 83% to 18% from delta front mouth bar—distal bar—shallow lake underwater uplift beach bar facies.

4.6 Features of high-quality reservoirs

The reservoirs with porosity of >15% and permeability of >10 mD were generally referred to as high-quality reservoirs in this paper.

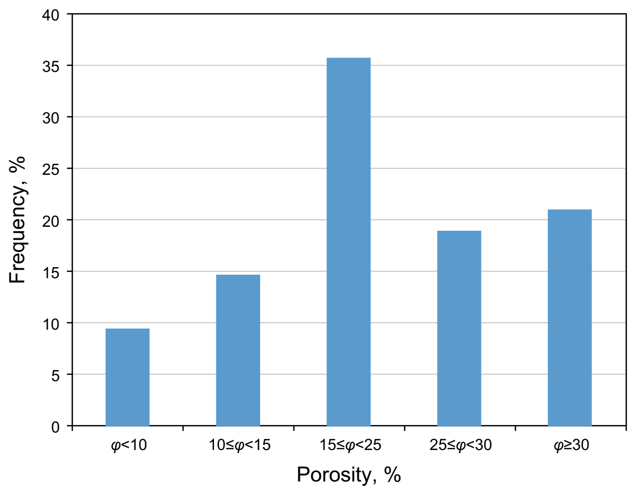

Fig. 4 Porosity distribution histogram of E_2s mixed siliciclastic–carbonate sediments

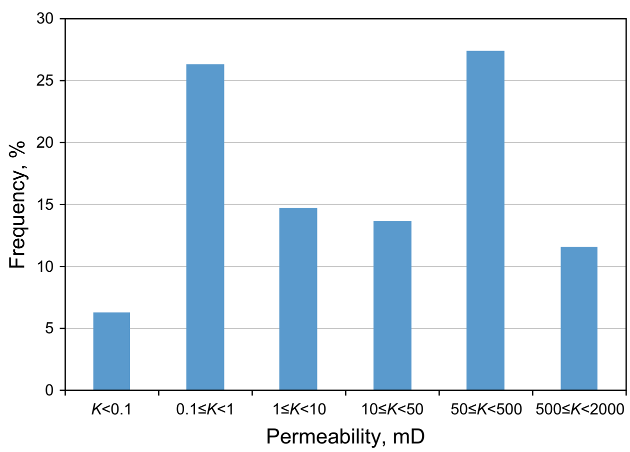

Fig. 5 Permeability distribution histogram of E_2s mixed siliciclastic–carbonate sediments

The sedimentary microfacies and the corresponding 106 groups of petrophysical data of the coring interval in Well HD2 and HD5, as well as the petrophysical data of the 50 sidewall cores of the other wells showed that the mixed siliciclastic–carbonate sediments developed in mouth bar, distributary river channel, and underwater beach bar microfacies had good physical properties, but high-quality reservoirs were basically not developed in the other microfacies (Fig. 7). Seventy-six percentage of the high-quality reservoirs were developed in Class I mixed siliciclastic–carbonate sediments, and their porosity and bioclastic content had good positive correlation (Fig. 8). Seventeen percentage of the high-quality reservoirs occurred in Class II mixed siliciclastic–carbonate sediments, and only 7% high-quality reservoirs occurred in Class III mixed siliciclastic–carbonate sediments. For diagenetic features, the vast majority of high-quality reservoirs were composed of pore-lining dolomite (Fig. 3a), with minor authigenic calcite. The mixed siliciclastic–carbonate sediments with pore-filling dolomite (Fig. 3c) and calcite were poor in physical properties. Dissolution was common in Class II mixed siliciclastic–carbonate sediments. Through comparing the reservoir space of high-quality reservoirs and poor-quality reservoirs, it can be seen that Class I mixed siliciclastic–carbonate sediments were dominated by primary porosity, such as intrafossil pores, followed by residual intergranular primary pores (Fig. 3a), while Class II mixed siliciclastic–carbonate sediments were dominated by residual intergranular primary and dissolved porosity.

5 Discussion

5.1 Genesis of primary pore development

Primary pores were pervasive in high-quality mixed siliciclastic–carbonate sedimentary reservoirs, especially in the reservoirs of Class I mixed siliciclastic–carbonate sediments. According to statistics of the microscopic pore type and plane porosity of the 87 cast thin sections of Class I mixed siliciclastic–carbonate sediments and 20 cast thin sections of Class II mixed siliciclastic–carbonate sediments, the primary plane porosity of Class I accounted for 90% of the total, while the primary plane porosity of Class II accounted for 42% of the total. The sedimentary microfacies of different types of mixed siliciclastic–carbonate sediments indicate that rocks were formed due to the mixed deposition of the siliciclastic grains and matrix in fan delta facies, and the carbonate particles and micrite deposited in the lacustrine facies. Carbonate particles mainly occurred in lacustrine high-energy underwater beach bars far away from terrigenous provenance, so that Class I mixed sediments with low micrite content and high primary intergranular porosity were well developed, whereas terrigenous clastics were common in the mouth bars near terrigenous provenance, so that Class II mixed sediments with low matrix content were developed.

Sixty-four percentage of carbonate particles were bioclasts. The bioclastic content and reservoir porosity showed a positive correlation in the study area (Fig. 8), since a large amount of intrafossil pores were formed due to biological decay. Most intrafossil pores were well preserved during burial process, so intrafossil pores are well developed in rocks (Fig. 3a). Thus, the bioclasts in the high-quality reservoirs in Class I mixed sediments contributed largely to the primary porosity.

Pore-lining dolomites were common in high-quality reservoirs, and they represented the formation features of vadose zone–phreatic zone as indicated by blade- and overhang-shaped distribution features. The analytical

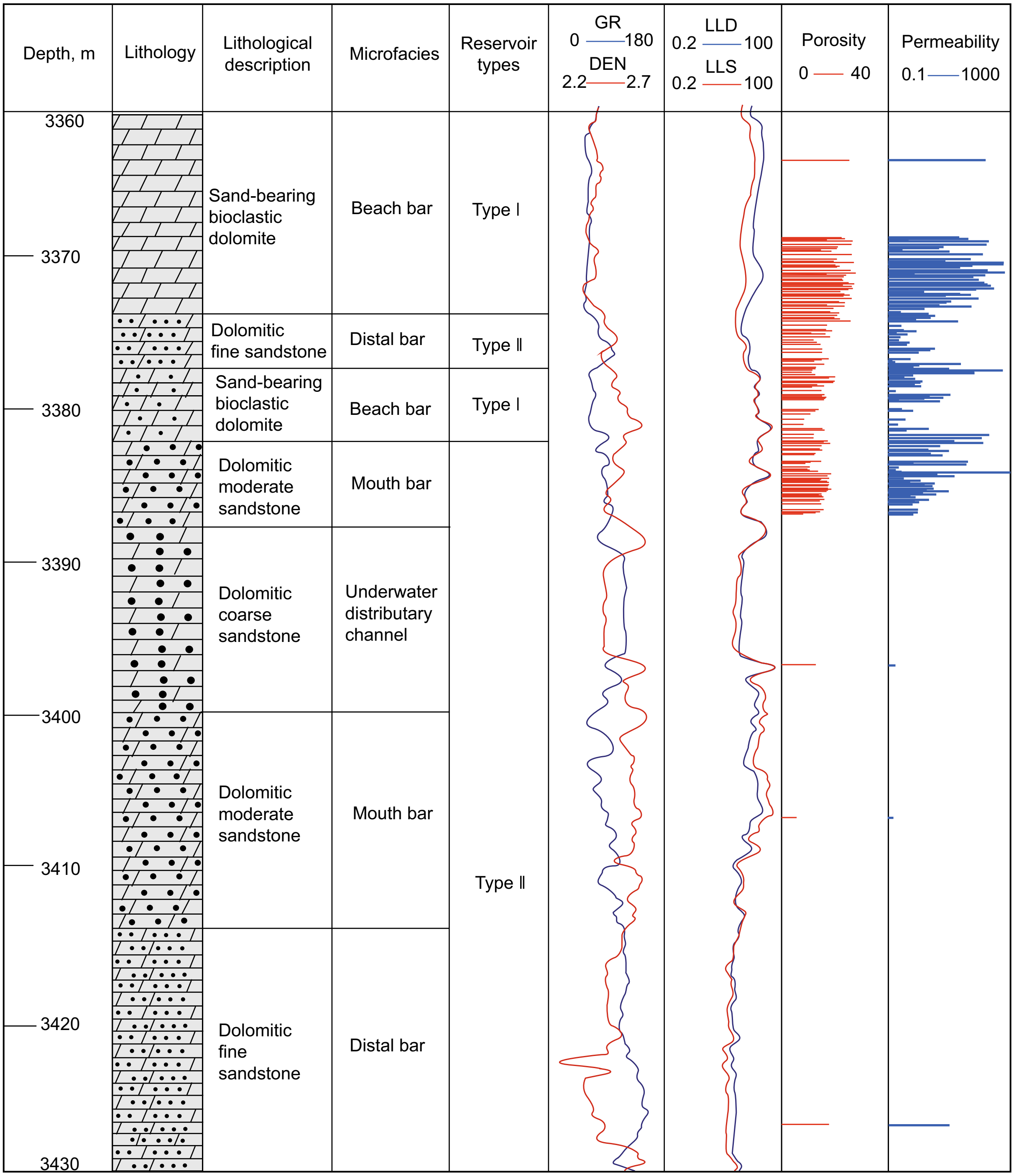

Fig. 6 Sedimentary microfacies of HD5 mixed siliciclastic–carbonate sedimentary interval (3360–3430 m)

results of isotopic temperatures (Table 1) showed that pore-lining dolomite was formed at a temperature of 29–83°C; together with the geothermal gradient of this region (Liu et al. 2012), it is inferred that the pore-lining dolomite in stage 1 (the earliest stage) was formed at a paleoburial depth of less than 150 m and the liner dolomite in stage 3 (the latest stage) was formed at a paleoburial depth of less than 1700 m and the pore-lining dolomites were formed early. It is indicated by the microscopic observation of early pore-lining dolomite development in reservoirs that the compaction was not strong. Under the burial condition of 4000 m, the point-line contact in grains was ubiquitously seen and the primary pores were well developed (Fig. 3a). By comparing the mixed siliciclastic–

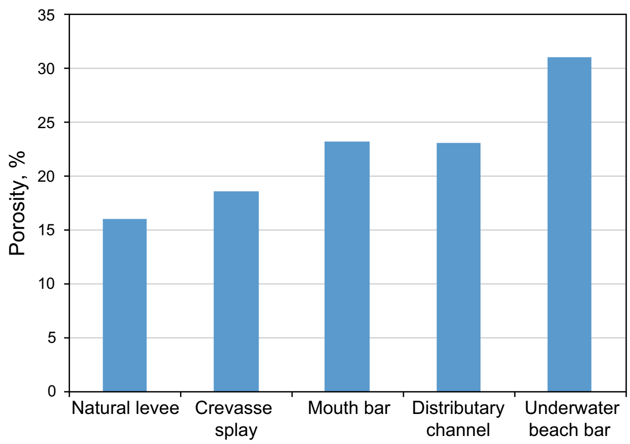

Fig. 7 Physical properties of different sedimentary microfacies of E_2s mixed siliciclastic–carbonate sediments

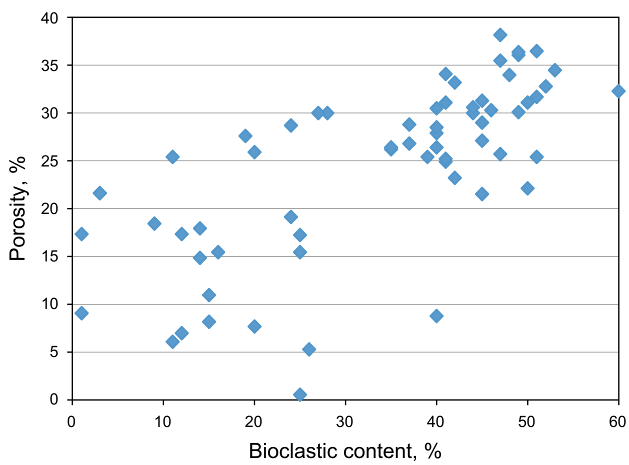

Fig. 8 Relation between the bioclastic content and porosity of E_2s mixed siliciclastic–carbonate sediments

carbonate sediments with and without pore-lining in early stage, it can be seen that the rocks without development of pore-lining in early stage mostly represented line contact, with low primary porosity (Fig. 3c). Therefore, the formation of the pore-lining dolomites in early stage effectively weakened the destruction of compaction on pores and was favorable to the preservation of intergranular primary pores.

5.2 Genesis of dissolved pore development

The dissolved pores were well developed in E_2s Class II mixed siliciclastic–carbonate sediments. The statistics of the pore types and content of 20 cast thin sections showed that the plane porosity of dissolved pores accounted for 58%. The crystal optical features of dissolved minerals showed that the dissolved minerals were mainly feldspar. Furthermore, the microprobe component analysis results of erosion remnants confirmed that the dissolved minerals were mainly albite and K-feldspar (Table 2). In addition, the authigenic clay minerals were kaolinite and illite, indicating that dissolution took place under a K-rich condition, resulting in the further transformation from kaolinite to illite (Zhang et al. 2007). The inclusion temperature of the authigenic quartz in mixed sedimentary reservoirs ranged between 122–143°C, and the authigenic quartz was formed due to the dissolution of feldspar. Thus, it is inferred that the dissolution of feldspar took place from late middle diagenetic stage to early epidiagenetic stage. The temperature ranges coincided with the temperature ranges of organic matter maturity stage, indicating that the abundant acidic fluids were discharged during organic matter evolution which had created conditions for the formation of dissolved pores in feldspar (Meng et al. 2010; Cao et al. 2014).

5.3 Early phase and multiphased hydrocarbon charging on pores

The microscopic fluorescence features of E_2s mixed sediments reflected multistage hydrocarbon charging features. For example, residual primary pores and intragranular dissolved pores had two types of completely different fluorescence, indicating at least two stages of hydrocarbon charging. The early stage residual intergranular primary pore showed yellow fluorescence, and the late stage showed green fluorescence, which was mainly from the dissolved pores in oolite (Fig. 3b). Hydrocarbon components were detected in the inclusions in temperature range of 73–87°C and 119–129°C with laser Raman (Table 3), indicating at least two stages of hydrocarbon charging.

Table 1 C and O isotope distribution of the pore-lining dolomite in E_2s mixed siliciclastic–carbonate sediments

Well	Well depth, m	Sample attribute	δ^{13}C PDB, ‰	δ^{18}O PDB, ‰	Formation temperature, °C	Formation buried depth, m
HD2	3382.1	Pore-lining dolomite in Stage 1	4.7	−0.76	29.4	126.70
HD2	3762.6	Pore-lining dolomite in Stage 2	5.41	−3.99	47.3	636.58
HD5	3375.06	Pore-lining dolomite in Stage 2	1.88	−4.01	47.4	639.99
HD5	3380.25	Pore-lining dolomite in Stage 2	2.02	−4.97	53.3	807.78
HD5	3375.65	Pore-lining dolomite in Stage 3	−0.42	−9.35	83.3	1666.86

Table 2 Probe composition distribution of the dissolved feldspar remnants in E_2s mixed siliciclastic–carbonate sediments

Well	Well depth, m	Na_2O	K_2O	Cr_2O_3	Al_2O_3	CaO	MnO	MgO	SiO_2	FeO	NiO	TiO_2	Mineral
HD5	3340.8	0.6	14.0	0.0	19.1	0.4	0.8	0.8	62.0	2.0	0.1	0.2	K-feldspar
HD5	3367.5	0.3	16.1	0.0	18.7	0.0	0.1	0.1	64.4	0.3	0.0	0.0	K-feldspar
HE3	3321.4	0.8	15.7	0.1	17.9	0.0	0.0	0.0	65.4	0.1	0.0	0.0	K-feldspar
HE3	3321.4	3.5	12.0	0.0	18.3	0.1	0.0	0.0	65.9	0.2	0.0	0.0	K-feldspar
HE3	3320.8	0.4	16.9	0.0	18.5	0.0	0.0	0.0	64.1	0.1	0.0	0.0	K-feldspar
HD2	3324.4	0.9	15.8	0.0	19.4	0.0	0.0	0.0	63.9	0.0	0.0	0.0	K-feldspar
HD2	3324.4	0.8	15.9	0.0	19.2	0.0	0.0	0.0	64.0	0.0	0.1	0.0	K-feldspar
HD2	3326	0.4	16.3	0.0	18.0	0.0	0.0	0.0	65.2	0.1	0.0	0.0	K-feldspar
Z13	3762.6	11.6	0.0	0.0	19.2	0.0	0.0	0.0	69.2	0.0	0.0	0.0	Albite
Z13	3762.6	11.8	0.0	0.1	19.2	0.0	0.0	0.0	68.9	0.0	0.0	0.0	Albite
Z13	3762.6	11.4	0.1	0.0	19.1	0.0	0.0	0.0	69.4	0.0	0.0	0.0	Albite
Z13	3762.6	11.6	0.1	0.0	19.2	0.0	0.0	0.0	69.1	0.0	0.0	0.0	Albite
BZ3	3779.2	11.7	0.1	0.0	19.3	0.2	0.0	0.0	68.6	0.1	0.0	0.0	Albite
BZ3	3779.2	11.5	0.0	0.0	19.1	0.2	0.0	0.0	69.2	0.0	0.0	0.0	Albite
BZ3	3779.2	11.6	0.0	0.0	19.4	0.1	0.0	0.0	68.9	0.0	0.0	0.0	Albite

Table 3 Gas phase components of the inclusions in E_2s mixed siliciclastic–carbonate sedimentary reservoirs

Well	Well depth, m	Gas phase, %						Host minerals	Homogenization temperature, °C
		CO_2	H_2S	CH_4	N_2	H_2	Total		
HD5	3382.1	0	0	35.7	0	64.3	100.0	Pore-lining dolomite of Stage 3	119
HD5	3370.05	0	16.1	20.8	63.1	0	100.0	Filling dolomite within oolite	73
HD5	3382.1	0	0	9.5	90.5	0	100.0	Pore-lining dolomite within intergranular pores	87
HD5	3383.1	78.1	0	21.9	0	0	100.0	Filling dolomite within intergranular pores	129
HD2	3454.98	51.2	0	7.3	41.5	0	100.0	Quartz enlarging	122

Combined with the paleogeothermal gradient in the study area, it is inferred that the reservoirs were buried at less than 1500 m when there was hydrocarbon charging at the earliest time. Generally, the early hydrocarbon charging can inhibit cementation and also reduced further compaction. Thus, the pores in reservoirs were effectively preserved (Meng et al. 2010; Cao et al. 2014).

6 Conclusions

The E_2s high-quality mixed siliciclastic–carbonate sedimentary reservoirs in the central Bohai Sea were deposited in a fan delta-lacustrine environment. The rocks were formed due to the mixed deposition of the siliciclastic material in fan deltas and carbonate particles deposited in lacustrine environments. The mixed sediment content of the carbonates gradually increased from a near provenance region to lacustrine underwater high-energy beach bars. The E_2s high-quality mixed siliciclastic–carbonate sedimentary reservoir rocks are mainly developed in Class I, followed by Class II. The development of the high-quality reservoirs of Class I siliciclastic–carbonate sediments was mainly controlled by a high-energy depositional environment, high bioclastic content and pore-lining dolomite and hydrocarbon charging in the early stage. Primary pores were developed in the underwater uplift beach bars with strong hydrodynamic conditions and low micrite content. Intrafossil pores were common due to soft biological decay, forming the main reservoir space of the high-quality reservoir rocks of Class I. The development of early stage pore-lining dolomite effectively weakened the destruction of mechanical compaction on pores. The hydrocarbon charging in the early stage effectively preserved reservoir pores. The development of the high-quality reservoirs of Class II mixed siliciclastic–carbonate sediments was mainly controlled by high-energy depositional environments, feldspar dissolution, pore-lining dolomite and hydrocarbon charging in the early stage. The intergranular primary pores were formed in a high-energy environment, such as fan delta front mouth bars and underwater distributary channels. Feldspar dissolution further improved reservoir properties. The hydrocarbon charging in the early stage and the formation of pore-lining dolomites effectively reduced the destruction of mechanical compaction on pores. Therefore, the E_2s mixed siliciclastic–carbonate sediments in the central Bohai Sea had good geological conditions for high-quality reservoir accumulation, and it is prospective for exploration and development.

Acknowledgements This work was financially supported by the National Science & Technology Specific Project (Grant No. 2011ZX05023-006).

References

Anan TI. Facies analysis and sequence stratigraphy of the Cenomanian–Turonian mixed siliciclastic–carbonate sediments in west Sinai, Egypt. Sediment Geol. 2014;307:34–6. doi:10.1016/j.sedgeo.2014.04.006.

Brandano M, Tomassetti L, Bosellini F, et al. Depositional model and paleodepth reconstruction of a coral-rich, mixed siliciclastic–carbonate system: the Burdigalian of Capo Testa (northern Sardinia, Italy). Facies. 2010;56(3):433–44. doi:10.1007/s10347-009-0209-1.

Campbell AE. Shelf-geometry response to changes in relative sea level on a mixed carbonate–siliciclastic shelf in the Guyana Basin. Sediment Geol. 2005;175(1–4):259–75. doi:10.1016/j.sedgeo.2004.09.003.

Cao YC, Yuan GH, Li XY, et al. Characteristics and origin of abnormally high porosity zones in buried Paleogene clastic reservoirs in the Shengtuo area high porosity zones in buried Paleogene clastic reservoirs in the Shengtuo area, Dongying Sag, East China. Pet Sci. 2014;11(3):346–62. doi:10.1007/s12182-014-0349-y.

Caracciolo L, Gramigna P, Critelli S, et al. Petrostratigraphic analysis of a Late Miocene mixed siliciclastic–carbonate depositional system (Calabria, Southern Italy): implications for mediterranean paleogeography. Sediment Geol. 2012;284–285:117–32. doi:10.1016/j.sedgeo.2012.12.002.

Feng JL, Cao J, Hu K, et al. Dissolution and its impacts on reservoir formation in moderately to deeply buried strata of mixed siliciclastic–carbonate sediments, northwestern Qaidam Basin, northwest China. Mar Pet Geol. 2013;39(1):124–37. doi:10.1016/j.marpetgeo.2012.09.002.

Feng JL, Cao J, Hu K, et al. Formation mechanism of middle-deep mixed rock reservoirs in the Qaidam basin. Acta Pet Sin. 2011a;27(8):2461–72 **(in Chinese)**.

Feng JL, Hu K, Cao J, et al. A review on mixed rocks of terrigenous clastics and carbonates and their petroleum-gas geological significance. Geol J China Univ. 2011b;17(2):297–307 **(in Chinese)**.

García-Hidalgo J, Gil J, Segura M, et al. Internal anatomy of a mixed siliciclastic–carbonate platform: the Late Cenomanian-Mid Turonian at the southern margin of the Spanish Central System. Sedimentology. 2007;54(6):1245–71. doi:10.1111/j.1365-3091.2007.00880.x.

Ge ZD, Wang XZ, Zhu M, et al. Reservoir characteristics of Archean magmatic rocks in the Dongying Sag. Lithol Reserv. 2011;23(4):48–52 **(in Chinese)**.

Guan DY, Wei G, Wang YC, et al. Controlling factors of middle-to-deep reservoir in Bozhong depression, Bohai Sea: an example from Shahejie formation in the steep slope belt of eastern Shijiutuo uplift. Nat Gas Explor Dev. 2012;35(2):5–8 **(in Chinese)**.

Guo XW, Liu KY, He S, et al. Petroleum generation and charge history of the northern Dongying Depression, Bohai Bay Basin, China: insight from integrated fluid inclusion analysis and basin modelling. Mar Pet Geol. 2012;32(1):21–35. doi:10.1016/j.marpetgeo.2011.12.007.

Hu ZW, Huang SJ, Li ZM, et al. Preliminary application of the dolomite-calcite oxygen isotope thermometer in studying the origin of dolomite in Feixianguan Formation, Northeast Sichuan, China. J Chengdu Univ Technol (Science & Technology Edition). 2012;39(1):1–9 **(in Chinese)**.

Liu DL, Tao SZ, Zhang BM. Application and questions about ascertaining oil-gas pools age with inclusions. Nat Gas Geosci. 2005;16(1):16–9 **(in Chinese)**.

Liu Z, Zhu WQ, Sun Q, et al. Characteristics of geotemperature-geopressure systems in petroliferous basins of China. Acta Pet Sin. 2012;27(2):1–17 **(in Chinese)**.

Liu ZG, Zhou XH, Li JP, et al. Reservoir characteristics and controlling factors of the Paleogene Sha-2 member in the 36-3 structure, Eastern Shijiutuo uplift, Bohai Sea. Oil Gas Geol. 2011;32(54):832–8 **(in Chinese)**.

Lubeseder S, Redfern J, Boutib L. Mixed siliciclastic-carbonate shelf sedimentation-Lower Devonian sequences of the SW Anti-Atlas, Morocco. Sediment Geol. 2009;215(1–4):13–32. doi:10.1016/j.sedgeo.2008.12.005.

Lu XL. Cenozoic faulting and its influence on the hydrocarbon-bearing systems hydrocarbon distribution in the Bohai Bay Basin. Pet Geol Recover Effic. 2005;12(3):31–5 **(in Chinese)**.

Lü ZX, Ye SJ, Yang X, et al. Quantification and timing of porosity evolution in tight sand gas reservoirs: an example from the Middle Jurassic Shaximiao Formation, western Sichuan. China Pet Sci. 2015;12(2):207–17. doi:10.1007/s12182-015-0021-1.

Ma YP, Liu L. Sedimentary and diagenetic characteristics of paleogene lacustrine mixed siliciclastic–carbonate sediments in the beach district, Dagang. Acta Sedimentol Sin. 2003;21(4):607–13 **(in Chinese)**.

Meng YL, Liang HW, Meng FJ, et al. Distribution and genesis of the anomalously high porosity zones in the middle-shallow horizons of the northern Songliao Basin. Pet Sci. 2010;7(3):302–10. doi:10.1007/s12182-010-0072-2.

Moissette P, Cornée J, Mannaï-Tayech B, et al. The western edge of the Mediterranean Pelagian Platform: a Messinian mixed siliciclastic–carbonate ramp in northern Tunisia. Palaeogeogr Palaeoclimatol Palaeoecol. 2010;285(1–2):85–103. doi:10.1016/j.palaeo.2009.10.028.

Mount JF. Mixing of siliciclastic and carbonate sediments in shallow shelf environments. Geology. 1984;12(7):432–5. doi:10.1130/0091-7613(1984)12<432:MOSACS>2.0.CO;2.

Ni JE, Sun LC, Gu L, et al. Depositional patterns of the 2nd member of the Shahejie Formation in Q oilfield of the Shijiutuo Uplift, Bohai Sea. Oil Gas Geol. 2013;34(4):491–8 **(in Chinese)**.

Palermo D, Aigner T, Geluk M, et al. Reservoir potential of a lacustrine mixed carbonate/siliciclastic gas reservoir: the lower

Triassic Rogenstein in the Netherlands. J Pet Geol. 2008;31(1):61–96. doi:10.1111/j.1747-5457.2008.00407.x.

Sha QA. Discussion on mixed deposits and mixed siliciclastic-carbonate rock. J Palaeogeogr. 2001;3(3):63–6 **(in Chinese)**.

Song ZQ, Chen YF, Du XF, et al. Study on sedimentary characteristics and reservoir of second member of Shahejie Formation, a structural area, Bohai sea. Offshore Oil. 2013;33(4):13–8 **(in Chinese)**.

Tian Y, Ying CC, Yan ZW, et al. The coupling of dynamics and permeability in the hydrocarbon accumulation period controls the oil-bearing potential of low permeability reservoirs: a case study of the low permeability turbidite reservoirs in the middle part of the third member of Shahejie. Pet Sci. 2016;13(2):204–24. doi:10.1007/s12182-016-0099-0.

Tong KJ, Zhao CM, Lü ZB, et al. Reservoir evaluation and fracture characterization of the metamorphic buried hill reservoir in Bohai Bay Basin. Pet Explor Dev Online. 2012;39(1):62–9. doi:10.1016/S1876-3804(12)60015-9.

Wang YB, Xue YA, Wang GY, et al. Shallow layer hydrocarbon accumulation characteristics and their exploration significances in Shijiutuo uplift, Bohai sea. China Offshore Oil Gas. 2015;27(2):8–16 **(in Chinese)**.

Xiao XM, Wei Q, Gai HF, et al. Main controlling factors and enrichment area evaluation of shale gas of the Lower Paleozoic marine strata in south China. Pet Sci. 2015;12(4):573–86. doi:10.1007/s12182-015-0057-2.

Xu W, Cheng KY, Cao ZL, et al. Original mechanism of mixed sediments in the saline lacustrine basin. Acta Pet Sin. 2014;30(6):1804–16 **(in Chinese)**.

Zand-Moghadam H, Moussavi-Harami R, Mahboubi A, et al. Comparison of tidalites in siliciclastic, carbonate, and mixed siliciclastic-carbonate systems: examples from Cambrian and Devonian deposits of East-Central Iran. ISRN Geol. 2013;2013:1–22. doi:10.1155/2013/534761.

Zhang JL, Jia Y, Du GL. Diagenesis and its effect on reservoir quality of Silurian sandstones, Tabei area, Tarim Basin, China. Pet Sci. 2007;4(3):1–13. doi:10.1007/s12182-007-0001-1.

Zhang NS, Reng XJ, Wei JX, et al. Rock types of mixed-sediment reservoirs and oil-gas distribution in Nanyishan of the Qaidam Basin. Acta Pet Sin. 2006;27(1):42–6 **(in Chinese)**.

Zhang YK, Hu XQ, Niu T, et al. Controlling of paleogeomorpology to Paleogene sedimentary systems of the Shijiutuo uplift in the Bohai Basin. J Jilin Univ Earth Sci Ed. 2015;45(6):1589–96 **(in Chinese)**.

Zonneveld JP, Gingras MK, Beatty TW et al (2012) Mixed siliciclastic/carbonate systems. In: Developments in sedimentology (Eds), vol 64, pp 807–3. doi:10.1016/B978-0-444-53813-0.00026-5.